Optimal chemotaxis in intermittent migration of animal cells

P. Romanczuk and G. Salbreux

Phys. Rev. E **91**, 042720 — Published 30 April 2015

DOI: 10.1103/PhysRevE.91.042720

Optimal chemotaxis in animal cell intermittent migration

P. Romanczuk[1,2], G. Salbreux[2]
[1] *Department of Ecology and Evolutionary Biology, Princeton University, NJ 80544, USA,*
[2] *Max Planck Institute for the Physics of Complex Systems, Nöthnitzerstr. 38, 01187 Dresden, Germany*
(Dated: March 26, 2015)

Animal cells can sense chemical gradients without moving, and are faced with the challenge of migrating towards a target despite noisy information on the target position. Here we discuss optimal search strategies for a chaser that moves by switching between two phases of motion ('run' and 'tumble'), reorienting itself towards the target during tumble phases, and performing persistent migration during run phases. We show that the chaser average run time can be adjusted to minimize the target catching time or the spatial dispersion of the chasers. We obtain analytical results for the catching time and for the spatial dispersion in the limits of small and large ratios of run time to tumble time, and scaling laws for the optimal run times. Our findings have implications for optimal chemotactic strategies in animal cell migration.

Eukaryotic cells migration does not always occur continuously: bimodal motions with reorientation phases where cells loose their polarity and phases of polarized, persistent motion have been reported in unicellular organisms [1], in cell migration occurring during development in the Zebrafish and Xenopus embryo [2–5], or in mammalian cells [6]. These two phases of motions have been denominated runs and tumbles [2] in analogy with *E. Coli* motion, although the corresponding migration mechanisms and chemical sensing of animal cells are very different to the ones employed by bacteria. Possibly, cellular run and tumble behavior reflects the necessity for the cell to retract motile protrusions before forming new ones [2]: in that case, the run time is associated to the protrusion lifetime (cf. Fig 1A).

Primordial germ cells (PGCs) in the Zebrafish embryo in particular have been reported to switch between two behavioural modes denoted "run" and "tumbles" [2]. In addition, PGCs move collectively in response to the chemokine SDF-1a towards the gonad during the first 24 hours of development [2]. In contrast to bacteria, after a tumble phase, PG cells choose a direction biased towards their target: animal cells are indeed capable of migration towards a source through sensing of chemical gradients [7, 8], allowing them to bias their motion towards a chemical source [9, 10] without the need to sample the chemoattractant at different spatial positions.

PG cells therefore display intermittent, directed migration towards a target. We investigate here the chemotactic efficiency of this class of motion with a minimal model. We ask in particular (i) how does the time necessary to find the target depend on the properties of the cell motion, and (ii), how does the spatial dispersion of a group of cells evolve in time. Both questions are relevant for biological processes, where cells have to move to specific locations and maintain their cohesion [11].

In random search processes, a chaser without information on the target location performs a random walk until hitting the target by chance [12, 13]. In this context, the persistence length of a particle performing a random search can be optimised to minimise the search time [14]. In this work, we consider instead the optimal moving strategy for another class of motion, directed random search, where the chaser has noisy information on the location of the target, and needs to slow down to reorient. More specifically, we consider an intermittent moving chaser which stops for a finite time to reorient towards its target (e.g. due to chemotaxis), with some detection error. This simple model accounts for the general situation where the reorientation of the chasing agent takes time, either due to physical constraints or to a finite detection time.

The main question is: how often should such a particle stop and reorient to efficiently move towards the target? Intuitively, short runs have the advantage of frequent reorientation towards the target, but at the cost of frequent stopping, while long runs may significantly deviate the particle from the location of the target, due to initial orientation errors and possible motion of the target. We show here that this results in an optimal run time which depends on the size and distance of the target and on the orientation errors that the chaser makes. Similarly, the effective diffusion of a collection of chasers can also be optimized, which might be essential for collective cell migration.

We consider point-like agents (chasers) moving in two dimensions towards a disc-shaped target with radius S located at position $\mathbf{x}_T$ (Fig. 1). The chaser position is denoted $\mathbf{x}_C$ and its direction of motion is given by the heading angle φ. The chasing agent switches between a run and a tumbling state. The tumbling phase lasts for a time t_t during which the chaser does not move, after which the agent picks a direction $\mathbf{u}_C$ towards the target, with an additional angular "detection" error η (Fig. 1). The initial polar angle of the chaser at the start of the run phase then reads

$$\varphi_i = \arg(\mathbf{x}_T - \mathbf{x}_C) + \eta. \tag{1}$$

For simplicity, η is drawn from a normal distribution with standard deviation ϵ. In general, the detection error ϵ might depend on the distance to the target d, for instance due to the spatial variation of the chemoattractant. In this work, we focus mainly on the simplest case of a constant ϵ, and relax this assumption at the end. During the

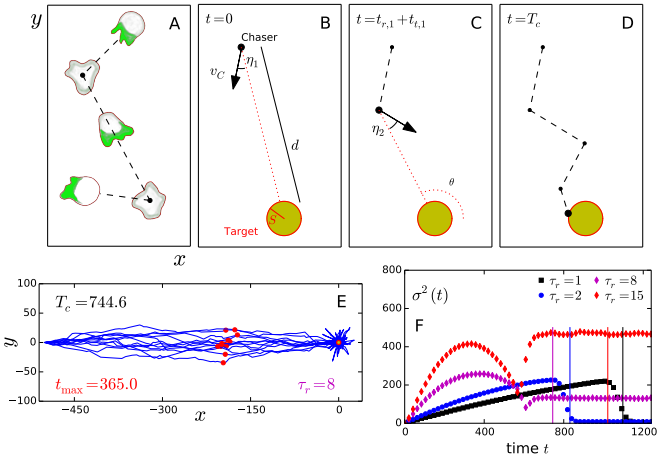

FIG. 1. (Color online) (A) Run and tumble migration of animal cells: Runs correspond to directed migration, of polarized cells with actin-rich protrusions (lamellipodia) at the leading edge (green). Tumbles correspond to reorientation events associated with repolarization events. (B-D) Model schematic: A chasing particle aims at a target by switching between persistent motion towards the target (runs) and reorientation events (tumbles). After reorientation, the chaser orients itself towards the target with an error η. (E) Simulation snapshot of 20 chaser trajectories for $\tau_r = 8$ and $t < T_c = 744.6$; the red (grey) circles indicates chaser positions at maximal dispersion ($t_{\max} = 388.0$). (F) Dispersion $\sigma^2(t)$ versus time for different run times. The vertical lines with the same colors indicate the corresponding average catching time T_c. Parameters (E,F): $\theta_0 = \pi$, $d_0 = 500$, $\epsilon = 0.3$, $S = 0.1$, $N = 40000$.

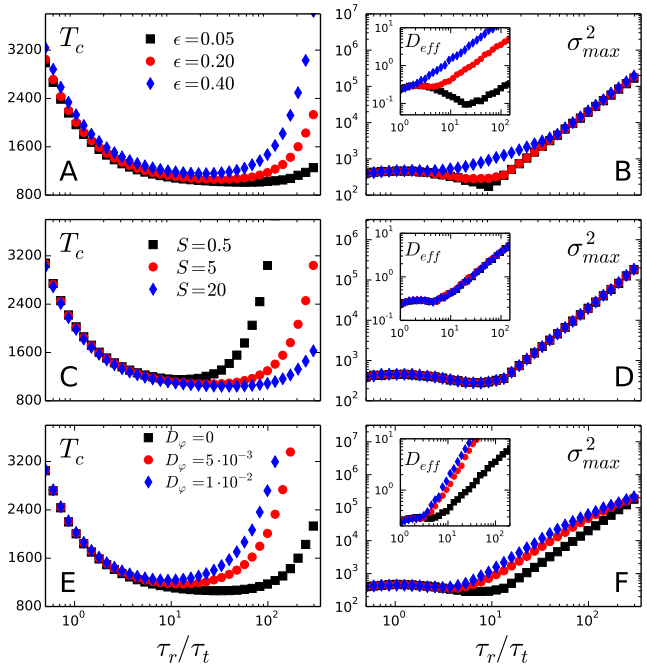

FIG. 2. (Color online) Catching time T_c (A,C,E) and maximum dispersion $\sigma^2_{\max}$ (B,D,F) versus τ_r/τ_t for different orientation errors ϵ (A,B), target radius S (C,D) and angular noise D_φ (E,F); insets show the effective diffusion coefficient $D_{\rm eff} = \sigma^2_{max}/t_{max}$. Default parameters: $N = 10^4$, $\theta_0 = \pi$, $\epsilon = 0.2$, $d_0 = 1000$, $\tau_t = 1$, $v_C = 1$, $S = 1$, $D_\varphi = 0$.

run phase lasting for a time t_r, the particle is not able to further bias its motion towards the target, and moves with a constant speed v_C and heading angle dynamics $\dot\varphi = \eta_C(t)$, with $\eta_C(t)$ a Gaussian white noise with variance D_φ. For $D_\varphi = 0$ the chaser moves on a straight line in the direction initially chosen $\varphi = \varphi_i$, whereas for $D_\varphi > 0$ it performs a persistent random walk.

We assume here random switching between the run and reorientation phases to be given by a dichotomous Markov process. The durations of the different phases, t_r and t_t, are exponentially distributed with an average run time τ_r and an average stopping time τ_t.

To gain insight in the dynamics of the chasing motion, we performed simulations of the motion of a collection of chasers (Fig. 1). At time $t = 0$ the chaser particles are placed at an angle θ_0 and distance d_0 from the target placed at the origin, $\mathbf{x}_T = 0$. Each chaser starts with a run with initial heading given by Eq. 1. Timescales are set by the tumbling time τ_t, velocities are normalized by the chaser velocity v_C and distances by $v_C\tau_t$.

To characterize the motion of chasers, we numerically evaluate the average catching time T_c and the spatial dispersion in chaser positions, $\sigma^2(t) = \langle(\mathbf{x}_C(t))^2\rangle - \langle\mathbf{x}_C(t)\rangle^2$. The dispersion exhibits different regimes over time (Fig. 1, [15]): an initial diffusive spread, where $\sigma^2(t)$ increases roughly linearly, is followed by a transition to a stationary state, where $\sigma^2(t)$ assumes a constant value.

We then evaluated the average catching time T_c, the maximum dispersion during the catching process $\sigma^2_{\max}$, and the initial effective diffusion $D_{\rm eff} = \sigma^2_{\max}/t_{\max}$ with $t_{\max}$ being the time of maximum dispersion. When varying the ratio of run to tumble time τ_r/τ_t, we observe that T_c is minimal for an optimal value of τ_r/τ_t (Fig. 2). $\sigma^2_{\max}$ also exhibits a minimum for zero or a finite value of the run time τ_r. This behavior can be understood intuitively as follows: for short run times τ_r, the chaser reorients frequently, allowing it to follow accurately the target; the frequent reorientations however slow the chaser down. For long run times on the other end, the chaser has a high probability to miss the target due to orientation errors, leading to large displacements away from the target. When varying the rotational diffusion of the chaser D_φ, we find that for $\tau_r > 1/D_\varphi$ the chaser "forgets" its initial direction during each run and the catching time sharply increases, while for short run times the catching time and chaser dispersion are unchanged (Fig. 2). Because rotational diffusion then essentially introduces a maximum value of τ_r above which the catching process becomes undirected, we focus on the limit $D_\varphi \to 0$ in the following.

To understand the origin of the optimal behavior, we note that two regimes emerge from the analysis of nu-

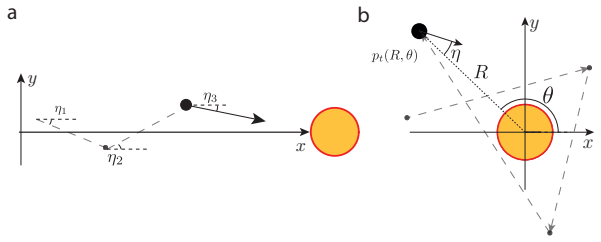

FIG. 3. (Color online) Limit cases of the chaser motion. (a) For small enough runs and away from the target, the chaser undergoes a nearly one-dimensional motion. (b) For large runs and close to the target, the chaser moves around the target and has a fixed probability of hitting the target at each run.

merical simulations depending on the ratio between the average run length and the distance to the target (Fig. 3). For $v_c\tau_r \ll |\mathbf{x}_C|$ (large distances and short runs), the chasing motion is dominated by a slow effective drift towards the target. For $v_c\tau_r \gtrsim |\mathbf{x}_C|$ (small distances and large runs), the chasers approach the vicinity of the target and the catching process is primarily dominated by the probability of hitting the target within a single run. The total catching time is then the sum of the time to approach the target (first regime), and the time to catch it (second regime). A visualization of the catching process for different average run times is provided in the Supplementary Material [15].

Based on these observations, we start by considering the limit of short runs with chasers positioned far from the target with the initial distance $d_0 \gg S$. We assume here, without loss of generality due to rotational symmetry, that the chaser initial position is along the x axis, $\mathbf{x}_c(t=0) = -d_0\mathbf{e}_x$. The chaser then follows a nearly one-dimensional motion along the x-direction, such that the desired chaser heading angle is small ($\varphi \approx 0$). The system can be described in terms of the spatial probability density functions (PDFs) for chaser particles in the run and tumble phase $p_r(\mathbf{x},\varphi)$ and $p_t(\mathbf{x})$ [16, 17], where the probability distribution is conditioned to the initial position and angle $(\mathbf{x}_0,\varphi_0)$. The general evolution equations for the PDFs in the frame of the target read

$$\partial_t p_r(\mathbf{x},\varphi) = -\mathbf{u}_r.\boldsymbol{\nabla} p_r(\mathbf{x},\varphi) - \frac{1}{\tau_r}p_r(\mathbf{x},\varphi) + \frac{1}{\tau_t}T(\varphi)p_t(\mathbf{x}) \tag{2}$$

$$\partial_t p_t(\mathbf{x}) = -\frac{1}{\tau_t}p_t(\mathbf{x}) + \frac{1}{\tau_r}\int_0^{2\pi} d\varphi p_r(\mathbf{x},\varphi), \tag{3}$$

where $\mathbf{u}_r = v_C\mathbf{u}_C(\varphi)$ is the drift velocity in the run phase, $T(\varphi) = \frac{1}{\sqrt{2\pi\epsilon}}\exp\left(-\frac{\varphi^2}{2\epsilon^2}\right)$ is the probability of reorientation in the φ direction after a tumble, $\boldsymbol{\nabla}$ denotes the gradient operator acting on the $\mathbf{x}$ dependency of $p_r(\mathbf{x},\varphi)$, and the time dependency of p_r and p_t is implicitly implied.

By deriving moment equations from Eqs. 2-3, we find that the average chaser velocity towards the target relaxes in a time $\tau_r\tau_t/(\tau_r+\tau_t)$ to the stationary value (Appendix A)

$$\langle v\rangle = \frac{v_C\tau_r e^{-\frac{\epsilon^2}{2}}}{\tau_r+\tau_t}, \tag{4}$$

while the chaser dispersion $\sigma^2(t) = D_{\text{eff}}t$ is predicted to increase linearly in time with the effective diffusion coefficient

$$D_{\text{eff}} = \frac{2v_C^2\tau_r^2}{\tau_r+\tau_t}\left[1-(1-\frac{\tau_t^2}{(\tau_r+\tau_t)^2})e^{-\epsilon^2}\right]. \tag{5}$$

For $\epsilon = 0$, $D_{\text{eff}} = \frac{2v_C^2\tau_r^2\tau_t^2}{(\tau_r+\tau_t)^3}$: in that limit, the diffusion is only due to the stochasticity in run and tumble times, and for large run time the diffusion constant decreases with τ_r, since each additional run introduces dispersion by generating different run lengths between different chasers (a zero run time also minimizes the diffusion, but the catching time then diverges). For $\epsilon \neq 0$, there is an optimal run time minimizing the diffusion coefficient, given for $\epsilon \to 0$ by $\tau_r/\tau_t = 1/\epsilon$: large runs indeed increase dispersion, because they tend to amplify initial errors in the heading angle.

The average approach time to the target is given in that drift-dominated limit by

$$T_c^{(1)} = \frac{d_0 - S}{v_C\frac{\tau_r}{\tau_r+\tau_t}e^{-\frac{\epsilon^2}{2}}}, \tag{6}$$

which agrees with numerical simulations (Fig. 6). Therefore, in the limit of small runs, increasing the run time is always favorable.

We now discuss the opposite limit when the target is sufficiently close to the chaser to be reached within a single run (Fig. 3B). We assume that the probability distribution of the chaser position at tumble, p_t, has relaxed to a steady state. The steady-state distribution is then isotropic. At lowest order in the orientation error ϵ, the chaser-target distance $R = |\mathbf{x}_c|$ is distributed according to an exponential distribution, $p_t(R) = \frac{1}{\tau_r v_c}e^{-\frac{R}{\tau_r v_c}}$, with the corresponding standard deviation of chaser position $\sigma_{\text{stat}} = \tau_r v_c$. To evaluate the catching time, we note that the probability of hitting the target in one run, after each tumble, is given by

$$p_{hit} = \int_{R=0}^{\infty} dR p_t(R)p_{\text{dir}}(R)p_{\text{reach}}(R), \tag{7}$$

where $p_{\text{dir}}(R)$ is the probability of choosing a direction towards the target, and $p_{\text{reach}}(R)$ is the probability of performing a sufficiently long run to actually reach the target. We start by evaluating p_{dir}. The chaser is heading towards the target provided that the detection error is sufficiently small, $|\eta| < S/R$ for small error ϵ. As a result, the probability of choosing the right direction by

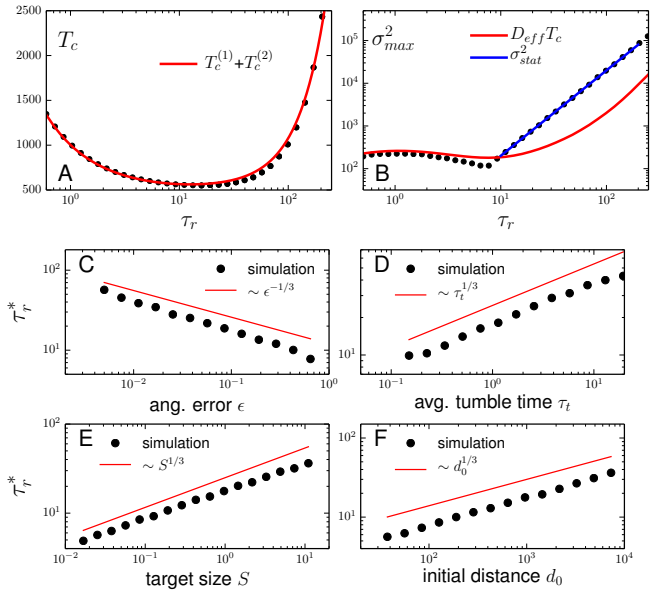

FIG. 4. (Color online) Comparison of simulation results and theory: (A) T_c and analytical prediction $T_c = T_c^{(1)} + T_c^2$; (B) $\sigma^2_{\max}$ with $D_{\rm eff}T_c$ for the "quasi-1D" approach and $\sigma^2_{\rm stat} = (\tau_r v_c)^2$ for the "single run" encounter (right). Parameters: $N = 10^4$, $\epsilon = 0.1$, $S = 1$, $d_0 = 500$. Scaling of the optimal run time τ_r^* minimizing T_c, (C) with the angular error ϵ, (D) the average tumble time τ_t, (E) the target size S and (F) the initial distance d. The solid lines indicate the predicted dependence from theory. Simulation parameters: $N = 10^4$, $v_T = 0.1$, and unless parameters are varied, $\tau_t = 1$, $v_C = 1$, $\epsilon = 0.2$, $S = 1$, $d_0 = 500$ and $\theta_0 = \pi$.

a favorable choice of error η is given by

$$p_{\rm dir}(R) = 2\int_0^{\frac{S}{R\sqrt{2}\epsilon}} dx \frac{e^{-x^2}}{\sqrt{\pi}}. \qquad (8)$$

To obtain $p_{\rm reach}(R)$, we note that (1) at lowest order in $\frac{S}{R}$, the run time has to to be larger than $t_{\rm catch} = R/v_C$ to reach the target, and (2) run times are taken out of an exponential distribution; therefore, $p_{\rm reach} = e^{-R/\tau_r v_C}$.

Overall, we then obtain $p_{\rm hit} \simeq \frac{1}{2} M(\frac{\sqrt{2}S}{\tau_r v_C \epsilon}) e^{\frac{S}{\tau_r v_C}}$ with $M(x) = \int_0^\infty dy\, e^{-y} {\rm Erf}(x/y)$ (Appendix B). Here, $M(x)$ is a monotonously increasing function of its argument and has limits $M(x) \simeq \frac{2}{\sqrt{\pi}} x \log\frac{1}{x}$ for $x \to 0$, and $M(x) \simeq 1$ for $x \to \infty$. The average catching time from the vicinity of the target reads

$$T_c^{(2)} \simeq \frac{2(\tau_r + \tau_t)}{M(\frac{\sqrt{2}S}{\tau_r v_C \epsilon})} e^{-\frac{S}{\tau_r v_C}}. \qquad (9)$$

Therefore, in the limit of large runs, decreasing the run time is favorable, an opposite behavior to the short run time limit discussed before.

The total time to reach the target, T_c, is the sum of the time required to approach the target (Eq. 6) and the time

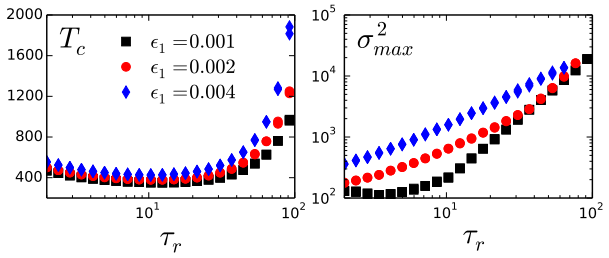

FIG. 5. (Color online) Catching time T_c and maximum dispersion $\sigma^2_{\max}$ versus ϵ_1. Simulation parameters: $N = 10^4$, $\tau_t = 1$, $v_C = 1$, $\epsilon_0 = 0.1$, $S = 1$, $d_0 = 300$ and $\theta_0 = \pi$.

to catch it in its vicinity (Eq. 9), $T_c = T_c^{(1)} + T_c^{(2)}$ (Appendix D). The resulting analytic prediction accounts very well for the catching time obtained by simulations (Fig. 4a). To estimate the optimal run time, we look for the minimum of the total catching time T_c. We find that for intermediate orientation error $S/\sqrt{d_0 v_c \tau_t} \ll \epsilon \ll 1$, the optimal run time τ_r^* scales approximately as (Appendix C)

$$\tau_r^* \sim \left(\frac{d_0 S}{v_c^2 \epsilon}\tau_t\right)^{1/3}. \qquad (10)$$

The condition can be rewritten as an optimal run length $\tau_r^* v_C \sim (d_0 S \tau_t v_c/\epsilon)^{\frac{1}{3}}$, scaling with the geometric mean of the three lengths of the problem. The predicted scaling appears verified by numerical simulations (Fig. 4c-f). The intermittent directed chaser has an optimal run length strikingly different from the optimal persistence length of a random searcher, which was found to be of the order of the system size [14]. It further implies that performing short length runs is better for small target sizes, when the distance to the target is close, and for short tumbles. The optimal run length is also crucially dependent on the orientation error: quite naturally, smaller orientation errors allow to perform larger runs.

In the minimal model discussed so far, we have assumed that the reorientation error ϵ is independent of the distance to the target $d(t) = |\mathbf{x_c}(t)|$. For directional sensing however, the detection accuracy of the target direction is likely to decrease with $d(t)$. To account for this, we numerically investigated an extension of our model by assuming that an arbitrary error function $\epsilon(d)$ can be approximated by a linear function $\epsilon(d) \approx \epsilon_0 + \epsilon_1 d$ with $\epsilon_1 > 0$. Simulations results for a finite ϵ_1 show the same qualitative behavior as the minimal model (Fig. 5): an optimal run time minimizing the catching time still exists. When increasing ϵ_1, the optimal run time minimizing the dispersion moves towards zero, similar to increasing the overall constant error ϵ (Fig. 2b).

We have also considered the situation where the target moves balistically with a finite, but small, speed $v_T < v_C$, and found that the same qualitative findings hold (Appendix E). A crucial difference for a finite target

speed v_T is the existence of a regime where the catching time T_c diverges, occurring above a threshold detection error ϵ or for short run time τ_r.

The robustness of our qualitative results to these modifications suggests that the minimal model introduced here exhibits physical properties which will be preserved for more realistic description of cells moving with intermittent motion. Developmental processes require cell migration occurring at the scale of the organism [18]: it would be interesting to experimentally test whether migrating cells operate near the optimum value predicted by Eq. 10 in this context. Recently, Minina *et al.* [3] have analyzed in detail guided migration of progenitor cell in vivo. Based on their experimental results they suggest that progenitor cells might adaptively decrease their run length by down regulating receptor signaling close to the source of the relevant chemokine. A disruption of this control mechanism for run length was shown to hinder precise arrival of cells at the target. These empirical findings are confirmed by our theoretical work, in particular by the predicted decrease in optimal run length with decreasing distance to the target (Fig. 4f). This indeed suggests that PG cells have evolved complex chemotactic strategies for precise spatial and temporal arrival at target sites, to ensure successful development of the embryo. We expect that further research combining new quantitative experiments and more elaborate theoretical models will provide important insights into the mechanism and function of directed cell migration in living systems.

From a more general point of view with respect to theory of search processes, our simple but generic model can be viewed as an investigation of optimal directed search, which is fundamentally different from the random search processes predominantly studied up to date.

Acknowledgements We thank Ewa Paluch and Alba Diz-Muñoz for bringing cellular run and tumble motion to our attention and for stimulating discussions, and Vasily Zaburdaev for helpful comments on the manuscript. PR gratefully acknowledges the hospitality of the Kavli Institute for Theoretical Physics (UCSB). This research was supported in part by the National Science Foundation under Grant No. NSF PHY11-25915.

Appendix A: Quasi one-dimensional motion

We consider here the limit case where the chaser is at large distance from the target $|\mathbf{x}_C - \mathbf{x}_T| \gg \tau_r v_C$, such that the chaser performs nearly one-dimensional motion along the axis joining the chaser to the target (Fig. 3a). In the main text, we consider a fixed target located at the origin of the coordinate system. In this Appendix however, we assume a slightly more general situation where the target is moving at constant speed v_T along the x-axis ($\mathbf{v}_T = v_T \mathbf{e}_x$). The results for a fixed target are recovered in the limit $v_T = 0$. Furthermore, the chaser is assumed to be far away from the target, such that its position $\mathbf{x}_C = x_c \mathbf{e}_x + y_c \mathbf{e}_y$ verifies $x_C \ll x_T$ and $y_C \approx y_T$. The desired heading of the chaser will then be approximately along the x-axis, $\varphi = \arg(\mathbf{x}_T - \mathbf{x}_C) \approx 0$. Thus, at the beginning of each new phase the new desired heading is simply $\varphi = \eta$, where η, the orientation error, is drawn from a Gaussian distribution $T(\varphi)$ with mean $\varphi = 0$ and variance ϵ^2 ($T(\varphi) = \frac{1}{\sqrt{2\pi}\epsilon} \exp\left(-\frac{\varphi^2}{2\epsilon^2}\right)$).

For convenience, calculations are done in this Appendix in a reference frame moving with the target and with the origin located at the initial position of the chaser. Therefore, $d\mathbf{x}/dt$ denotes the velocity of the chaser in the referential of the target, and $\mathbf{x}(t=0) = 0$ is the initial position of the chaser. We denote by $p_r(\mathbf{x}, \varphi)$ the probability that the chaser is in a run phase at position $\mathbf{x}$ with heading angle φ, and by $p_t(\mathbf{x})$ the probability of it being in a tumble phase at position $\mathbf{x}$. These probabilities also depend on time, and this dependency is implicitly implied in the rest of these supplementary informations, if not explicitly stated otherwise. Since the chaser switches between run and tumbles with rates τ_r^{-1} and τ_t^{-1}, the master equation for these probability densities can be written

$$\partial_t p_r(\mathbf{x}, \varphi) = -\mathbf{u}_r . \boldsymbol{\nabla} p_r(\mathbf{x}, \varphi) - \frac{1}{\tau_r} p_r(\mathbf{x}, \varphi) + \frac{1}{\tau_t} T(\varphi) p_t(\mathbf{x}) \tag{A1}$$

$$\partial_t p_t(\mathbf{x}) = -\mathbf{u}_t . \boldsymbol{\nabla} p_t(\mathbf{x}) - \frac{1}{\tau_t} p_t(\mathbf{x}) + \frac{1}{\tau_r} \int_0^{2\pi} d\varphi p_r(\mathbf{x}, \varphi), \tag{A2}$$

where $\mathbf{u}_r = v_C \mathbf{u}_C(\varphi) - v_T \mathbf{e}_x$ and $\mathbf{u}_t = -v_T \mathbf{e}_x$ are the drift velocities respectively in the run and tumble phase, with $\mathbf{u}_C(\varphi) = \cos\varphi \mathbf{e}_x + \sin\varphi \mathbf{e}_y$ the direction of the chaser.

We now calculate the solution for the drift and velocity of the moving agent from Eqs. A1 and A2. To do so, we start by introducing the probability of being in a run $\rho_r = \int d\mathbf{x} d\varphi p_r(\mathbf{x}, \varphi)$ and the probability of being in a tumble $\rho_t = \int d\mathbf{x} p_t(\mathbf{x})$. It is then straightforward to obtain the time evolution of these two probabilities:

$$\partial_t \rho_r = -\frac{1}{\tau_r} \rho_r + \frac{1}{\tau_t} \rho_t \tag{A3}$$

$$\partial_t \rho_t = -\frac{1}{\tau_t} \rho_t + \frac{1}{\tau_r} \rho_r, \tag{A4}$$

which relaxes to the stationary solution $\rho_r = \frac{\tau_r}{\tau_r + \tau_t}$, $\rho_t = \frac{\tau_t}{\tau_r + \tau_t}$ within the time $\sim \frac{\tau_r \tau_t}{\tau_r + \tau_t}$. For convenience, we assume in this Appendix that initial conditions for the probability of being in a run or tumble are given by $\rho_r(t=0) = \frac{\tau_r}{\tau_r + \tau_t}$ and $\rho_t(t=0) = \frac{\tau_t}{\tau_r + \tau_t}$, such that the run and tumble probabilities are already at stationary state. The initial probability distribution p_r and p_t are then given by

$$p_r(\mathbf{x}, \varphi, t=0) = \frac{\tau_r}{\tau_r + \tau_t} \delta(\mathbf{x}) T(\varphi) \tag{A5}$$

$$p_t(\mathbf{x}, t=0) = \frac{\tau_t}{\tau_r + \tau_t} \delta(\mathbf{x}). \tag{A6}$$

We now introduce the average position during the runs $\langle \mathbf{x} \rangle_r$, the average position during the tumbles $\langle \mathbf{x} \rangle_t$, the average velocity during the runs $\langle \mathbf{v} \rangle_r$, and the average velocity during the tumbles $\langle \mathbf{v} \rangle_t$, given respectively by:

$$\langle \mathbf{x} \rangle_r = \frac{1}{\rho_r} \int d\mathbf{x} \int d\varphi \ \mathbf{x} p_r(\mathbf{x}, \varphi) \tag{A7}$$

$$\langle \mathbf{x} \rangle_t = \frac{1}{\rho_t} \int d\mathbf{x} \ \mathbf{x} p_t(\mathbf{x}) \tag{A8}$$

$$\langle \mathbf{v} \rangle_r = \frac{1}{\rho_r} \int d\mathbf{x} \int d\varphi \ \mathbf{u}_r p_r(\mathbf{x}, \varphi) \tag{A9}$$

$$\langle \mathbf{v} \rangle_t = \frac{1}{\rho_t} \int d\mathbf{x} \mathbf{u}_t p_t(\mathbf{x}). \tag{A10}$$

Using Eqs. A1 and A2, one arrives at the following set of equations for these quantities:

$$\partial_t(\rho_r \langle \mathbf{x} \rangle_r) = \rho_r \langle \mathbf{v}_r \rangle - \rho_r \frac{1}{\tau_r} \langle \mathbf{x} \rangle_r + \rho_t \frac{1}{\tau_t} \langle \mathbf{x} \rangle_t \tag{A11}$$

$$\partial_t(\rho_t \langle \mathbf{x} \rangle_t) = \rho_t \langle \mathbf{v}_t \rangle - \rho_t \frac{1}{\tau_t} \langle \mathbf{x} \rangle_t + \rho_r \frac{1}{\tau_r} \langle \mathbf{x} \rangle_r \tag{A12}$$

$$\partial_t(\rho_r \langle \mathbf{v} \rangle_r) = -\rho_r \frac{1}{\tau_r} \langle \mathbf{v} \rangle_r + \rho_t \frac{1}{\tau_t} \int d\phi T(\phi) \mathbf{u}_r(\phi) \tag{A13}$$

$$\partial_t(\rho_t \langle \mathbf{v} \rangle_t) = -\rho_t \frac{1}{\tau_t} \langle \mathbf{v} \rangle_t + \rho_r \frac{1}{\tau_r} \mathbf{u}_t. \tag{A14}$$

We now extract the long-time behaviour of the positions and velocities, after a transient relaxation occurring on a time $\max(\tau_r, \tau_t)$. The velocities then relax to the steady-state values

$$\langle \mathbf{v} \rangle_r = \int d\varphi T(\varphi) \mathbf{u}_r(\varphi) \simeq (v_C e^{-\frac{\epsilon^2}{2}} - v_T) \mathbf{e}_x \tag{A15}$$

$$\langle \mathbf{v} \rangle_t = \mathbf{u}_t = -v_T \mathbf{e}_x, \tag{A16}$$

and the average position $\langle \mathbf{x} \rangle = \rho_r \langle \mathbf{x} \rangle_r + \rho_t \langle \mathbf{x} \rangle_t$ follows the equation

$$\partial_t \langle \mathbf{x} \rangle = \rho_r \langle \mathbf{v} \rangle_r + \rho_t \langle \mathbf{v} \rangle_t = \langle \mathbf{v} \rangle, \tag{A17}$$

so that the particle moves along the x-axis with a constant drift velocity

$$\langle \mathbf{v} \rangle = \frac{\tau_r \int d\varphi T(\varphi) \mathbf{u}_r(\varphi) + \tau_t \mathbf{u}_t}{\tau_r + \tau_t} \simeq \left[\frac{v_C \tau_r e^{-\frac{\epsilon^2}{2}}}{\tau_r + \tau_t} - v_T \right] \mathbf{e}_x. \tag{A18}$$

The drift velocity relative to the target is positive only for $\frac{\tau_r}{\tau_t} > \frac{1}{\frac{v_C}{v_T} e^{-\frac{\epsilon^2}{2}} - 1}$; below this value, the drift is negative and the chaser does not reach the target. When the velocity is positive, the time to approach the vicinity of the target is given by

$$T_c^{(1)} = \frac{d_0 - S}{\langle \mathbf{v} \rangle} = \frac{d_0 - S}{\frac{v_C \tau_r e^{-\frac{\epsilon^2}{2}}}{\tau_r + \tau_t} - v_T}. \tag{A19}$$

We now turn to the calculation of the second moments:

$$\langle x^2 \rangle_r = \frac{1}{\rho_r} \int d\mathbf{x} \int d\varphi \ x^2 p_r(\mathbf{x}, \varphi) \tag{A20}$$

$$\langle x^2 \rangle_t = \frac{1}{\rho_t} \int d\mathbf{x} \ x^2 p_t(\mathbf{x}) \tag{A21}$$

$$\langle v^2 \rangle_r = \frac{1}{\rho_r} \int d\mathbf{x} \int d\varphi \ \mathbf{u}_r^2 p_r(\mathbf{x}, \varphi) \tag{A22}$$

$$\langle v^2 \rangle_t = \frac{1}{\rho_t} \int d\mathbf{x} \ \mathbf{u}_t^2 p_t(\mathbf{x}) \tag{A23}$$

$$\langle \mathbf{x} \cdot \mathbf{v} \rangle_r = \frac{1}{\rho_r} \int d\mathbf{x} \int d\varphi \mathbf{u}_r \cdot \mathbf{x} p_r(\mathbf{x}, \varphi) \tag{A24}$$

$$\langle \mathbf{x} \cdot \mathbf{v} \rangle_t = \frac{1}{\rho_t} \int d\mathbf{x} \mathbf{u}_t \cdot \mathbf{x} p_t(\mathbf{x}). \tag{A25}$$

Assuming that the densities and average velocities have relaxed to steady state, we find the following dynamic equations for the second moments:

$$\partial_t(\rho_r \langle x^2 \rangle_r) = 2\rho_r \langle \mathbf{x} \cdot \mathbf{v} \rangle_r - \frac{1}{\tau_r} \rho_r \langle x^2 \rangle_r + \frac{1}{\tau_t} \rho_t \langle x^2 \rangle_t \tag{A26}$$

$$\partial_t(\rho_t \langle x^2 \rangle_t) = 2\rho_t \langle \mathbf{x} \cdot \mathbf{v} \rangle_t - \frac{1}{\tau_t} \rho_t \langle x^2 \rangle_t + \frac{1}{\tau_r} \rho_r \langle x^2 \rangle_r \tag{A27}$$

$$\partial_t(\rho_r \langle \mathbf{x} \cdot \mathbf{v} \rangle_r) = \rho_r \langle v^2 \rangle_r - \frac{1}{\tau_r} \rho_r \langle \mathbf{x} \cdot \mathbf{v} \rangle_r + \frac{1}{\tau_t} \rho_t \langle \mathbf{v} \rangle_r \langle \mathbf{x} \rangle_t \tag{A28}$$

$$\partial_t(\rho_t \langle \mathbf{x} \cdot \mathbf{v} \rangle_t) = \rho_t \langle v^2 \rangle_t - \frac{1}{\tau_t} \rho_t \langle \mathbf{x} \cdot \mathbf{v} \rangle_t + \frac{1}{\tau_r} \rho_r \langle \mathbf{v} \rangle_t \langle \mathbf{x} \rangle_r \tag{A29}$$

$$\partial_t(\rho_r \langle v^2 \rangle_r) = -\frac{1}{\tau_r} \rho_r \langle v^2 \rangle_r + \rho_t \frac{1}{\tau_t} \int d\varphi u_r(\varphi)^2 T(\varphi) \tag{A30}$$

$$\partial_t(\rho_t \langle v^2 \rangle_t) = -\frac{1}{\tau_t} \rho_t \langle v^2 \rangle_t + \rho_r \frac{1}{\tau_r} u_t^2, \tag{A31}$$

where $u_r = |\mathbf{u}_r|$ and $u_t = |\mathbf{u}_t|$. Solving Eqs. A11-A14 and Eqs. A28-A31, we find that after a transient relaxation of order $\max(\tau_r, \tau_t)$, the last four correlations relax

to the steady state solutions

$$\langle v^2\rangle_r = \int d\phi u_r(\phi)^2 T(\phi) \simeq v_C^2 + v_T^2 - 2v_T v_C e^{-\frac{\epsilon^2}{2}} \quad \text{(A32)}$$

$$\langle v^2\rangle_t = u_t^2 = v_T^2 \quad \text{(A33)}$$

$$\langle \mathbf{x}\cdot\mathbf{v}\rangle_r = \tau_r\langle v^2\rangle_r + \langle \mathbf{v}\rangle_r \cdot \left[\langle \mathbf{v}\rangle(t-\tau_r) - \frac{\tau_r^2\tau_t}{(\tau_r+\tau_t)^2}(\langle \mathbf{v}\rangle_r - \langle \mathbf{v}\rangle_t)\right] \quad \text{(A34)}$$

$$\langle \mathbf{x}\cdot\mathbf{v}\rangle_t = \tau_t\langle v^2\rangle_t + \langle \mathbf{v}\rangle_t \cdot \left[\langle \mathbf{v}\rangle(t-\tau_t) + \frac{\tau_r\tau_t^2}{(\tau_r+\tau_t)^2}(\langle \mathbf{v}\rangle_r - \langle \mathbf{v}\rangle_t)\right]. \quad \text{(A35)}$$

Using these solutions and Eqs. A26-A27, we find that the total second moment $\langle x^2\rangle = \rho_r\langle x^2\rangle_r + \rho_t\langle x^2\rangle_t$ is then given for $t\to\infty$ by

$$\langle x^2\rangle = \langle \mathbf{v}\rangle^2 t^2 + 2t\Big[\rho_r\tau_r\langle v^2\rangle_r + \rho_t\tau_t\langle v^2\rangle_t - \frac{1}{\tau_r+\tau_t}\left(\tau_r^2\langle \mathbf{v}\rangle_r + \tau_t^2\langle \mathbf{v}\rangle_t\right)\cdot\langle \mathbf{v}\rangle + \frac{\tau_r\tau_t}{(\tau_r+\tau_t)^2}\left(\langle \mathbf{v}\rangle_r - \langle \mathbf{v}\rangle_t\right)\cdot \left(-\tau_r\rho_r\langle \mathbf{v}\rangle_r + \tau_t\rho_t\langle \mathbf{v}\rangle_t\right)\Big], \quad \text{(A36)}$$

and the dispersion therefore evolves in the long time limit as

$$\langle x^2\rangle - \langle \mathbf{x}\rangle^2 = 2t\Big[\rho_r\tau_r\langle v^2\rangle_r + \rho_t\tau_t\langle v^2\rangle_t - \frac{1}{\tau_r+\tau_t}\left(\tau_r^2\langle \mathbf{v}\rangle_r + \tau_t^2\langle \mathbf{v}\rangle_t\right)\cdot\langle \mathbf{v}\rangle + \frac{\tau_r\tau_t}{(\tau_r+\tau_t)^3}\left(\langle \mathbf{v}\rangle_r - \langle \mathbf{v}\rangle_t\right)\cdot\left(-\tau_r^2\langle \mathbf{v}\rangle_r + \tau_t^2\langle \mathbf{v}\rangle_t\right)\Big]. \quad \text{(A37)}$$

The effective diffusion $D_{\rm eff}$, defined by $\langle x^2\rangle - \langle \mathbf{x}\rangle^2 = D_{\rm eff}t$,

$$D_{\rm eff} = \frac{2v_C^2\tau_r^2}{\tau_r+\tau_t}\left[1 - (1 - \frac{\tau_t^2}{(\tau_r+\tau_t)^2})e^{-\epsilon^2}\right], \quad \text{(A38)}$$

is independent on the target velocity.

Appendix B: Single Run Catch

We discuss in this Appendix the limit where the chaser is close to the target and can reach it within a single run (Fig. 3B). To estimate the catching time, we evaluate the probability that the chaser is able to hit the target in a single run, $p_{\rm hit}$. In this Appendix, we assume as in the main text that the target is fixed at the origin. The chaser particle can now be located at any position in the plane around the target, and we use polar coordinates, $\mathbf{x}_C = R\cos\theta\mathbf{e}_x + R\sin\theta\mathbf{e}_y$. The problem is invariant by rotation around the target and all probability distribution functions are therefore independent of θ. We assume that the probability distribution of chaser positions at tumble, $p_t(R)$, has relaxed to steady-state. As stated in the main text, the hitting probability can then be written

$$p_{\rm hit} = \int_{R=0}^{\infty} dR p_t(R) p_{\rm dir}(R) p_{\rm reach}(R), \quad \text{(B1)}$$

where $p_{\rm dir}(R)$ is the probability of choosing a direction towards the target, and $p_{\rm reach}(R)$ is the probability of performing a sufficiently long run to actually reach the target. We now evaluate these different probabilities.

1. Stationary distribution of the chaser position at tumbles p_t

To obtain the stationary distribution of chaser positions around the target, we take the limit of vanishing error, ϵ (corrections to the stationary distribution introduce higher-order corrections in ϵ in the catching time $T_c^{(2)}$). The chaser is always aiming at the origin, and crosses it when, by chance, the run length is large enough. The master equation for the probability distribution of (tumbling) positions of the chaser $p_t(R,t)$ can then be written

$$p_t(R,t_{n+1}) = \int_{r=0}^{\infty} dr p(r+R) p_t(r,t_n) + \int_{r=R}^{\infty} dr p(r-R) p_t(r,t_n), \quad \text{(B2)}$$

with $p(r) = e^{-\frac{r}{\tau_r v_C}}/(\tau_r v_C)$ the probability of performing a run of length r. The first term on the right-hand side of Eq. B2 corresponds to trajectories crossing the target between $t=t_n$ and $t=t_{n+1}$, while the second term correspond to trajectories which do not cross it. Solving for the stationary distribution of the probability distribution of tumbling positions of the chaser, we find

$$p_t(R) = \frac{1}{\tau_r v_C}\left[\int_{r=0}^{\infty} dr e^{-\frac{r+R}{\tau_r v_C}} p_t(r) + \int_{r=R}^{\infty} dr e^{-\frac{r-R}{\tau_r v_C}} p_t(r)\right]. \quad \text{(B3)}$$

Differentiating twice this equation, one obtains

$$p_t''(R) = -\frac{1}{\tau_r v_C} p_t'(R), \quad \text{(B4)}$$

such that the solution of this differential equation is the exponential distribution

$$p_t(R) = \frac{1}{\tau_r v_C} e^{-\frac{R}{\tau_r v_C}}, \quad \text{(B5)}$$

so that the positions of the chaser at tumble are exponentially distributed away from the target, with a characteristic length $\tau_r v_C$.

2. Probability that the chaser runs towards the target $p_{\rm dir}$

We now consider the motion of the chaser towards the target, after a tumble, from position (R,θ). The target

position $\mathbf{x} = x\mathbf{e}_x + y\mathbf{e}_y$ then evolves according to

$$x(t) = R\cos\theta - v_C\cos(\theta+\eta)t \tag{B6}$$
$$y(t) = R\sin\theta - v_C\sin(\theta+\eta)t\ , \tag{B7}$$

with η the error in the orientation taken by the chaser. The chaser reaches the target when it crosses its boundary at time $t_{\rm catch}$:

$$x(t_{\rm catch})^2 + y(t_{\rm catch})^2 = S, \tag{B8}$$

Solving for this equation, we find that a solution exists for

$$|\sin\eta| < \frac{S}{R}. \tag{B9}$$

For $S = 0$, the only possible solution is indeed for $\eta = 0$, since in that case, the target is indeed reduced to a point, and the chaser direction has to go exactly through the origin. For small errors $\epsilon \ll 1$, one can approximate the condition B9 by $|\eta| < S/R$. Given that η is taken out of the Gaussian distribution (approximation of the von Mises distribution) $p(\eta) = \frac{1}{\epsilon\sqrt{2\pi}}e^{-\frac{\eta^2}{2\epsilon^2}}$, one can then evaluate the probability that a favorable direction is chosen towards the target

$$\begin{aligned} p_{\rm dir}(R,\theta) &= \frac{1}{\epsilon\sqrt{2\pi}}\int_{-\frac{S}{R}}^{\frac{S}{R}} e^{-\frac{\eta^2}{2\epsilon^2}}d\eta \\ &= {\rm Erf}\left(\frac{S}{R\sqrt{2}\epsilon}\right) \end{aligned} \tag{B10}$$

with ${\rm Erf}(x)$ the error function.

3. Probability of performing a sufficiently long run $p_{\rm reach}$

From Eq. B8, the catching time is given at lowest order in the error η by

$$t_{\rm catch} \simeq \frac{R-S}{v_C}. \tag{B11}$$

To reach the target, the chaser then has to perform a run lasting for a sufficiently long time, $t_r > t_{\rm catch}$. Because run times are taken out of an exponential distribution, the probability of performing a sufficiently long run, conditioned to the probability of a right choice of direction, is given by

$$p_{\rm reach}(R,\theta) = e^{-t_{\rm catch}/\tau_r}. \tag{B12}$$

4. Total hitting probability

From Eq. B1, we finally find the total hitting probability

$$\begin{aligned} p_{\rm hit} &= \frac{e^{\frac{S}{\tau_r v_C}}}{\tau_r v_C}\int_{R=0}^{\infty} dr{\rm Erf}\left(\frac{S}{r\sqrt{2}\epsilon}\right)e^{-\frac{2r}{\tau_r v_C}} \\ &= \frac{1}{2}\int_{x=0}^{\infty} dx e^{-x}{\rm Erf}\left(\frac{2S}{\tau_r v_C x\sqrt{2}\epsilon}\right)e^{\frac{S}{\tau_r v_C}} \\ &= \frac{1}{2}M\left(\frac{\sqrt{2}S}{\tau_r v_C\epsilon}\right)e^{\frac{S}{\tau_r v_C}}, \end{aligned} \tag{B13}$$

where we have introduced the function $M(a) = \int_{x=0}^{\infty} dx e^{-x}{\rm Erf}(a/x)$. Note that by using the expansion $M(a) \simeq \frac{2}{\sqrt{\pi}}a\log\frac{1}{a}$ for $a \to 0$, an even simpler expression can be obtained for the hitting probability in the limit of long runs, $\tau_r \gg S/(v_C\epsilon)$,

$$p_{\rm hit} \simeq \frac{\sqrt{2}}{\sqrt{\pi}}\frac{S}{\tau_r v_C\epsilon}\log(\frac{\tau_r v_C\sqrt{2}\epsilon}{S})\ . \tag{B14}$$

The average catching time can then be evaluated from $p_{\rm hit}$. The distribution of the number of runs done before catching N_c is $p(N_c) = p_{\rm hit}(1-p_{\rm hit})^{N_c-1}$. The average number of runs before catching is then $\langle N_c\rangle = 1/p_{\rm hit}$, and the average catching time is given by

$$T_c^{(2)} = \tau_r\langle N_c\rangle = \frac{\tau_r+\tau_c}{p_{\rm hit}} = \frac{2(\tau_r+\tau_t)}{M\left(\frac{\sqrt{2}S}{\tau_r v_C\epsilon}\right)}e^{-\frac{S}{\tau_r v_C}} \tag{B15}$$

Appendix C: Optimization of the total catching time

Using the results of Appendices A and B, the expression for the total catching time $T_c = T_c^{(1)} + T_c^{(2)}$ reads for $d_0 \gg S$:

$$T_c = \frac{d_0(\tau_r+\tau_t)}{v_C\tau_r e^{-\epsilon^2/2}} + \frac{2(\tau_r+\tau_t)}{M\left(\frac{\sqrt{2}S}{\tau_r v_C\epsilon}\right)}e^{-\frac{S}{\tau_r v_C}}. \tag{C1}$$

We now aim at giving a simple expansion for this catching time, in order to estimate the optimal run time τ_r minimizing T_c. In the limit where $\epsilon \gg S/(\tau_r v_C)$, the argument within the function M is much smaller than 1, and the function $M(a)$ can be expanded for small a:

$$M(a) \simeq \frac{2}{\sqrt{\pi}}a\log\frac{1}{a} + \frac{2\log 2 + \psi(3/2) - 2\gamma}{\sqrt{\pi}}a, \tag{C2}$$

with γ the Euler-Mascheroni constant and $\psi(x)$ the digamma function [19, 20]. With this expression, one obtains for the derivative of the catching time:

$$\begin{aligned} \frac{\partial T_c}{\partial\tau_r} \simeq &-\frac{d_0\tau_t}{v_C e^{-\epsilon^2/2}\tau_r^2} \\ &+\sqrt{2\pi}\epsilon\frac{v_C}{Sx^2}(2(x-1)\tau_r + (x-2)\tau_t). \end{aligned} \tag{C3}$$

where $x = \log \frac{2e^{\psi\left(\frac{3}{2}\right)-2\gamma} v_C^2 \epsilon^2 \tau_r^2}{S^2}$ a logarithmic function of τ_r, positive and larger than 1 in the regime $\epsilon \gg S/(\tau_r v_C)$ that we consider here. To solve for the optimal value of the run time τ_r^* minimizing the catching time , we assume a priori that $\tau_r^* \gg \tau_t$, giving then

$$\tau_r^{*3} = \frac{d_0 S \tau_t x^2}{2\sqrt{2\pi}(x-1) v_C^2 \epsilon e^{-\frac{\epsilon^2}{2}}}. \tag{C4}$$

We note that the coefficient x being a logarithmic function of τ_r, it varies weakly with τ_r and can be treated as constant for the purpose of obtaining approximate scaling properties. The resulting scaling for the optimal run time then reads for $\epsilon \ll 1$

$$\tau_r^* \sim \frac{(d_0 S \tau_t)^{\frac{1}{3}}}{v_C^{\frac{2}{3}} \epsilon^{\frac{1}{3}}}. \tag{C5}$$

This scaling has be obtained assuming that $\epsilon \gg S/\tau_r^* v_C$ and $\tau_r^* \gg \tau_t$: one can verify using Eq. C5 that these approximations are self-consistent for

$$\frac{S}{\sqrt{d_0 v_C \tau_t}} \ll \epsilon \ll \frac{d_0 S}{\tau_t^2 v_C^2}. \tag{C6}$$

In addition, $\epsilon \ll 1$, since we had previously assumed that the orientation error is small. In numerical simulations performed in the manuscript, the initial distance to the target d_0 is large enough to ensure $d_0 S \gg \tau_t^2 v_C^2$; therefore, the condition $\epsilon \ll 1$ is more stringent than the upper boundary in Eq. C6. Numerical estimates of the optimal run time indicate that the scaling Eq. C5 appears verified for the corresponding intermediate range of error $\frac{S}{\sqrt{d_0 v_C \tau_t}} \ll \epsilon \ll 1$ (Fig. 4).

Appendix D: Numerical simulations for the approach time

The analysis in Appendix C postulates that the catching time can be separated into two phases, such that the total catching time is the sum of the time to approach the target in a nearly one-dimensional motion, $T_c^{(1)}$, and the time to catch the target once the chaser is in its vicinity, $T_c^{(2)}$:

$$T_c = T_c^{(1)} + T_c^{(2)}. \tag{D1}$$

To verify that this separation holds, we note that the time to approach the target $T_c^{(1)}$ can be itself decomposed into the time to approach a sphere of radius $v_C \tau_r$ around the target, and the average time for the chasers to reach the target $v_C \tau_r / \langle \mathbf{v} \rangle$ (cf. Eq. A19)

$$T_c^{(1)} = T_{\text{approach}} + T_{\text{reach}}, \tag{D2}$$

where for a stationary target ($v_T = 0$, cf. Eq. A18):

$$T_{\text{approach}} = \left(\frac{d_0 - S}{v_C \tau_r} - 1 \right) (\tau_r + \tau_t) e^{\frac{\epsilon^2}{2}} \tag{D3}$$

$$T_{\text{reach}} = (\tau_r + \tau_t) e^{\frac{\epsilon^2}{2}} \ . \tag{D4}$$

T_{approach} can be, in contrast to $T_c^{(1)}$, directly measured in numerical simulations, as the mean first passage time of the chasers to circular region with the radius $v_C \tau_r$. From T_{approach} we can calculate $T_c^{(1)}$ using Eq. D2 and consequently obtain $T_c^{(2)}$ from subtracting $T_c^{(1)}$ from the total average catching time T_c: $T_c^{(2)} = T_c - T_c^{(1)}$. Thus by measuring T_{approach} and T_c simultaneously, we are able to verify our separation ansatz by comparing the simulation results with theory.

The theoretical predictions of our simple approach is in excellent agreement with estimates from numerical simulations (Fig. 6).

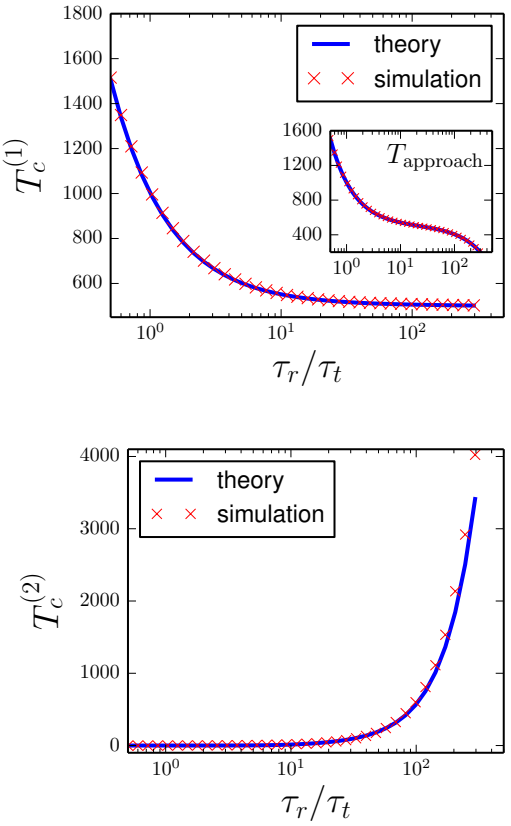

FIG. 6. (Color online) Comparison of the analytical results for $T_c^{(1)} = T_{\text{approach}} + T_{\text{reach}}$ (cf. Eq. D3) and $T_c^{(2)}$ with the results of numerical simulations. The inset shows the comparison for T_{approach}. (Parameters: $N = 10^4$, $\epsilon = 0.1$, $S/v_C\tau_t = 1$, $d_0/v_C\tau_t = 500$, $\theta_0 = \pi$)

Appendix E: Finite target velocity

To test whether our findings are robust when introducing a finite target velocity $\mathbf{v}_T = v_T \mathbf{e}_x$, we compared the theoretical predictions with simulation results for a target speed $v_T/v_C = 0.1$ (Fig 7). In Fig. 7, we used the analytical result for $T_c^{(1)}$ obtained in Appendix A for

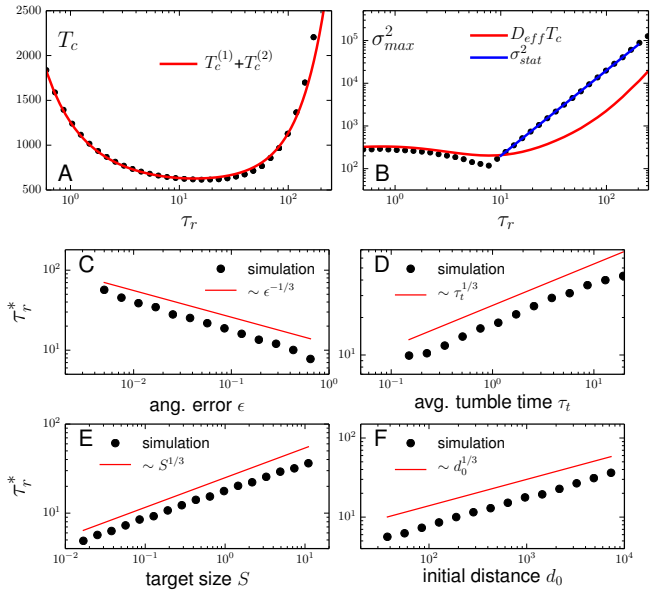

FIG. 7. (Color online) Comparison of simulation results and theory for a finite target speed $v_T/v_C = 0.1$: (A) T_c and analytical prediction $T_c = T_c^{(1)} + T_c^{(2)}$; (B) $\sigma^2_{\max}$ with $D_{\rm eff}T_c$ for the "quasi-1D" approach and $\sigma^2_{\rm stat} = (\tau_r v_C)^2$ for the "single run" encounter (right). Parameters: $N = 10^4$, $\epsilon = 0.1$, $S/v_C\tau_t = 1$, $d_0/v_C\tau_t = 500$. Scaling of the optimal run time τ_r^* minimizing T_c, (C) with the angular error ϵ, (D) the average tumble time τ_t, (E) the target size S and (F) the initial distance d. The solid lines indicate the predicted dependence from theory. Simulation parameters: $N = 10^4$, $v_T/v_C = 0.1$, and unless parameters are varied, $\tau_t = 1$, $v_C = 1$, $\epsilon = 0.2$, $S = 1$, $d_0 = 500$ and $\theta_0 = \pi$.

$v_T > 0$:

$$T_c^{(1)} = \frac{d_0 - S}{\langle \mathbf{v} \rangle} = \frac{d_0 - S}{\frac{v_C \tau_r e^{-\frac{\epsilon^2}{2}}}{\tau_r + \tau_t} - v_T}. \tag{E1}$$

Note that $T_c^{(1)}$ is positive only for τ_r sufficiently large, such that

$$\tau_r > \tau_r^d = \tau_t \frac{1}{\frac{v_C}{v_T} e^{-\epsilon^2/2} - 1}. \tag{E2}$$

Indeed, below this threshold, the drift velocity may become negative if the chaser is located behind the target, and in this case it can never reach the target.

[1] M. Polin, I. Tuval, K. Drescher, J. P. Gollub, and R. E. Goldstein, Science **325**, 487 (2009), PMID: 19628868.
[2] M. Reichman-Fried, S. Minina, and E. Raz, Developmental Cell **6**, 589 (2004).
[3] S. Minina, M. Reichman-Fried, and E. Raz, Current Biology **17**, 1164 (2007).
[4] H. Blaser, M. Reichman-Fried, I. Castanon, K. Dumstrei, F. L. Marlow, K. Kawakami, L. Solnica-Krezel, C.-P. Heisenberg, and E. Raz, Developmental Cell **11**, 613 (2006).
[5] E. Theveneau, L. Marchant, S. Kuriyama, M. Gull, B. Moepps, M. Parsons, and R. Mayor, Developmental Cell **19**, 39 (2010), PMID: 20643349.
[6] A. A. Potdar, J. Lu, J. Jeon, A. M. Weaver, and P. T. Cummings, Annals of biomedical engineering **37**, 230 (2009), PMID: 18982450 PMCID: PMC3586332.
[7] K. F. Swaney, C.-H. Huang, and P. N. Devreotes, Annual Review of Biophysics **39**, 265 (2010), PMID: 20192768.
[8] H. Levine and W.-J. Rappel, Physics Today **66**, 24 (2013).
[9] R. G. Endres and N. S. Wingreen, Proceedings of the National Academy of Sciences **105**, 15749 (2008).
[10] M. Ueda and T. Shibata, Biophysical Journal **93**, 11 (2007).
[11] M. Doitsidou, M. Reichman-Fried, J. Stebler, M. Köprunner, J. Dörries, D. Meyer, C. V. Esguerra, T. Leung, and E. Raz, Cell **111**, 647 (2002).
[12] V. Méndez, D. Campos, and F. Bartumeus, in *Stochastic Foundations in Movement Ecology*, Springer Series in Synergetics (Springer Berlin Heidelberg, 2014) pp. 177–205.
[13] O. Benichou, M. Coppey, M. Moreau, P.-H. Suet, and R. Voituriez, Physical Review Letters **94**, 198101 (2005).
[14] V. Tejedor, R. Voituriez, and O. Benichou, Physical Review Letters **108**, 088103 (2012).
[15] See Supplemental Material at [URL will be inserted by publisher] for Supplementary Movies.
[16] H. G. Othmer, S. Dunbar, and W. Alt, Journal of Mathematical Biology **26**, 263 (1988).
[17] F. Thiel, L. Schimansky-Geier, and I. M. Sokolov, Phys. Rev. E **86**, 021117 (2012).
[18] B. E. Richardson and R. Lehmann, Nature reviews. Molecular cell biology **11**, 37 (2010), PMID: 20027186.
[19] M. Abramowitz and I. A. Stegun, *Handbook of mathematical functions: with formulas, graphs, and mathematical tables*, 55 (Courier Dover Publications, 1972).
[20] I. Wolfram Research, *Mathematica*, version 9.0 ed. (Wolfram Research, Inc., 2012).